Liquid-crystal-based terahertz tunable Solc filter

I-Chen Ho,[1] Ci-Ling Pan,[1,*] Cho-Fan Hsieh,[2] and Ru-Pin Pan[2,3]

[1]*Department of Photonics and Institute of Electro-Optical Engineering, National Chiao Tung University, Hsinchu, Taiwan 30010*

[2]*Department of Electrophysics, National Chiao Tung University, Hsinchu, Taiwan 30010*

[3] *E-mail: rpchao@mail.nctu.edu.tw*

**Corresponding author: clpan@faculty.nctu.edu.tw*

Received February 13, 2008; revised May 14, 2008; accepted May 14, 2008;
posted May 19, 2008 (Doc. ID 92736); published June 19, 2008

A broadly tunable terahertz Solc-type birefringence filter is demonstrated. The first central passband frequency of the filter can be continuously tuned from 0.176 to 0.793 THz using magnetically controlled birefringence in nematic liquid crystals. The insertion loss of the present device is about 5 dB.

OCIS codes: 320.7080, 230.3720, 230.5440, 260.5430, 350.2460, 320.0320.

Quasi-optic [1] components, filters in particular, are in high demand owing to the recent rapid development and emerging applications of terahertz (THz) science and technology [2]. Several types of tunable THz filters have been demonstrated as of late. A cryogenic THz attenuator and filter, with a mixed type-I/type-II GaAs/AlAs multiple quantum well structure, was tuned by optical injection of carriers [3]. By using $SrTiO_3$ as a defect material, Nemac *et al.* [4] demonstrated a photonic crystal filter that could be temperature tuned from 185 to 100 GHz. Yang and Sambles [5] reported a voltage-controlled wavelength selection at microwave frequencies by using a grating structure with liquid crystals (LCs). A plasmonic filter was made tunable over the range of 365–386 GHz by a lateral shift of 140 μm between two micromachined metallic photonic crystal (MPC) plates [6]. Recently, Pan *et al.* [7] have demonstrated control of central frequency of enhanced THz transmission through a two-dimensional metallic hole array (2D-MHA) by controlling the index of refraction of the nematic LCs filling the holes adjacent to the 2D-MHA on one side. An LC-based tunable THz Lyot filter with a tunable range from 0.388 to 0.564 THz and a fractional tuning range of 40% were also reported [8].

The Solc filter [9,10], such as the Lyot filter, is a type of birefringence filter also widely employed in the visible near infrared and demonstrated for the millimeter wavelengths [11]. It consists of a stack of identical birefringence plates with folded azimuthal angles between crossed polarizers or fanned azimuthal angles between parallel polarizers. The Solc filter is inferior to the Lyot filter in the suppression of secondary maxima near the primary transmission bands. On the other hand, its bandwidth is slightly narrower, and its transparency is much better [12]. Solc filters can be made tunable using active birefringence retarders such as electro-optic (EO) crystals [13] or LC cells [14]. In this Letter, we have constructed and characterized a THz Solc filter using an LC as the birefringent phase plate.

A folded Solc filter [15] consists of a series of an even number of half-wave plates at central frequency f_c between crossed polarizers. Each of the wave plates is alternatively oriented at an azimuthal angle ρ and $-\rho$ with respect to the polarization direction of the incident electromagnetic wave. The central frequency f_c of the filter is given by

$$f_c = \frac{(2m+1)c}{2(n_e - n_o)d}, \quad m = 0,1,2,3, \ldots, \tag{1}$$

where n_o and n_e are the refractive indices of ordinary and extraordinary waves, respectively, d is the thickness of each wave plate, m is the order of the half-wave plates, and c is the speed of light in vacuum. Making use of the Jones matrix method and the identity of Chebyshev [15], we can write the transmittance of the filter as

$$T = \left| \tan 2\rho \cos\chi \frac{\sin N\chi}{\sin\chi} \right|^2. \tag{2}$$

In Eq. (2), $\cos\chi = \cos 2\rho \sin\Gamma/2$, where Γ is the frequency-dependent phase retardation of each plate and N is an even number and represents the number of plates. Furthermore, Eq. (2) reduces to $T = \sin^2 2N\rho$ when $\Gamma = (2m+1)\pi$. Thus, the transmittance of the filter at f_c is 100% if $\rho = \pi/4N$.

As schematically drawn in Fig. 1, a two-stage Solc filter was constructed with two LC tunable retarders (TRs) designed such that $\rho = 22.5°$. The TRs were placed between a pair of parallel wire-grid polarizers (Specac, GS57204). We adopted this geometry instead of the standard configuration with crossed polarizers because of experimental constraints by our photoconductive-antenna-based terahertz time-domain spectrometer (THz-TDS) [7] employed for characterization of the filter. As shown in the inset (a) in Fig. 1, the first of two types of LC-based TRs were of our previous design [8]. The LC cell in the TR was constructed with two fused-silica plates and filled with LC (E7, Merck), of which n_e and n_o are about 1.71 and 1.57 in the terahertz frequency range [16]. The substrates were coated with *N*,*N*-dimethyl-*n*-octadecyl-3-aminopropyltrimethoxysilyl chloride (DMOAP) for homeotropic alignment [17]. Thicknesses of the LC layers in both TRs were 5.7 mm, controlled by aluminum spacers. The thresh-

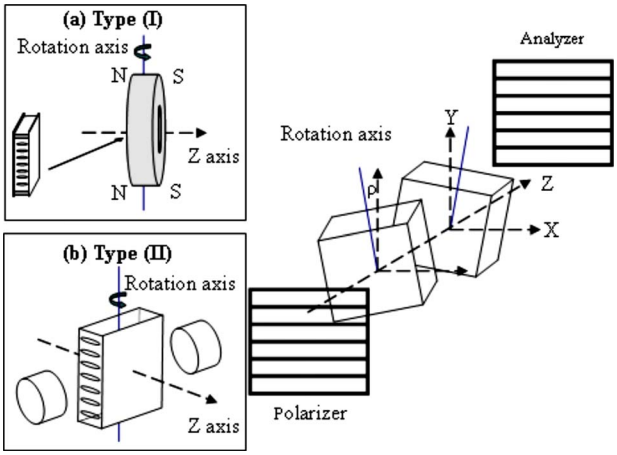

Fig. 1. (Color online) Schematic of the LC-based tunable THz Solc filter. The insets (a) and (b) show two different ways to apply the magnetic field on the same tunable LC THz retarders.

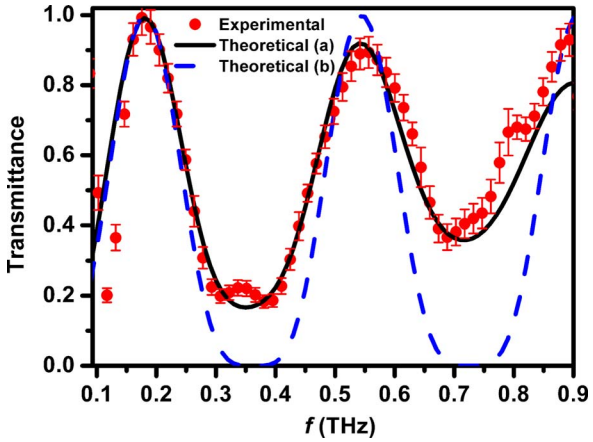

Fig. 2. (Color online) Example of the transmittance of the broadband THz pulse through the LC Solc filter. The circles are experimental data. The solid and dashed curves are theoretical predictions according to Eq. (2) (a) with and (b) without the unequal imaginary indices taken into account.

old field required to reorient LC molecules with the magnetic field perpendicular to the alignment direction is less than 0.001 T [18]. The maximum magnetic field at the cell position in the rotary permanent magnets (sintered Nd–Fe–B) is 0.427 T, ensuring that all LC molecules were parallel to the magnetic field. The retardation provided by each of the TRs is zero when the LC director is parallel to the z axis. By rotating the magnets, we achieve tunable retardation.

While rotating the magnets, the incident THz waves could be partially blocked by the rotating magnets. The range of rotation angle is from 0° to 45° for type I TRs. For larger angles, a second type is used. The type II TRs [see inset (b) in Fig. 1] consisted of the same LC cells but each with a pair of cylindrical magnets, which could also be rotated to achieve angles larger than 55°. The magnetic field strength at the position of the LC cell in this setup is 0.19 T, also large enough to align all LC molecules in the cell. The retardation provided by the TRs is at the maximum when the magnetic field is perpendicular to the z axis in type II TRs and decreases as the magnets are rotated about the LC cell.

Experimentally measured spectral transmittances of the device shown in Fig. 1 were normalized to that of a reference consisting of two E7 cells. The reference LC cells were identical to those used in the filter, except that their directors were parallel to the polarization of the incident THz wave. The data were then converted into that for the standard folded Solc filter with crossed polarizers. An example (type II, magnet rotation angle=90°) is shown in Fig. 2. The peak transmission frequencies for the zeroth, first, and second orders are 0.176, 0.556, and 0.892 THz, respectively. These are in good agreement with the theoretical prediction according to Eq. (1). As the rotation angle was turned from 90° to smaller angles, the terahertz spectrum transmitted by the filter shifted to higher frequencies. The bandwidth of the filter output at higher frequencies was larger than that of the lower one, while minimum transmittance is not equal to zero. This can be explained by the unequal imaginary parts of refractive indices for ordinary and extraordinary rays ($\kappa_o=0.020$, $\kappa_e=0.007$) of E7 [16]. Filtering by separation and recombination of polarization components is only partially effective. From the coupled mode theory [15], two orthogonally polarized normal modes are coupled in this quasi-periodic filter. For $\kappa_o \neq \kappa_e$, the phase matching condition will not be satisfied and energy cannot be completely exchanged from one mode to the other. Therefore, the contrast of our THz Solc filter is less than the ideal case. The theoretical values, solid and dashed curves in Fig. 2, plotted according to Eq. (2) with and without the unequal values of the imaginary indices taken into account, are also shown in Fig. 2. The solid curve is in excellent agreement with the experimental data.

The tunable behavior of the Solc filter is illustrated in Fig. 3. The zeroth-order central frequency of the type I Solc filter can be tuned from 0.794 to 0.474 THz by rotating the magnetic field from 30° to 45° with respect to the z axis, while the tuning range of the type II Solc filter is from 0.293 to 0.176 THz by

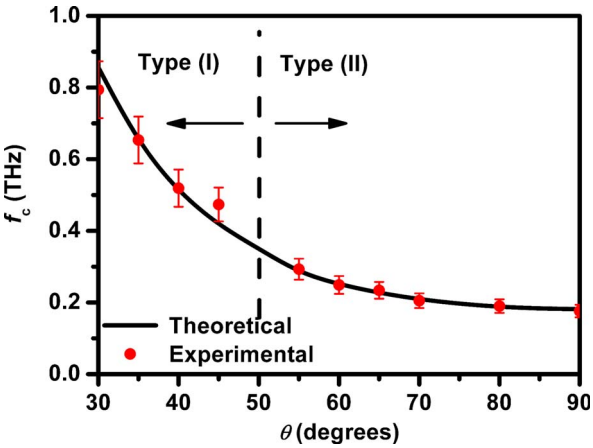

Fig. 3. (Color online) Zeroth-order central frequencies of the filter versus rotation angle θ between the magnetic field and the z axis. The circles are experimental data. The curve is the theoretical prediction according to Eq. (1).

rotating the magnetic field from 55° to 90°. The fractional tuning ranges are 67.5% and 66.5%, respectively. Thus the frequency tunability of THz LC Solc filter is significantly larger than that of the Lyot filter previously reported by us.

The typical waveform of a THz pulse transmitted through a Solc filter consisting of several peaks is shown in Fig. 4. The occurrence of multiple peaks can easily be understood as the following: The THz wave was separated into an *o*-ray and an *e*-ray after passing through the first LC cell, and these two waves were further split into *o*-*o*, *o*-*e*, *e*-*o*, and *e*-*e* components after traversing the second one. Moreover, the two LC cells were designed to have the same phase retardation so that the *e*-*o* and *o*-*e* components overlap each other. The *e*-*e* component, with the largest retardation, overlapped in time with the main signal of the reference (*e*-ray). The *o*-*o* components with the smallest retardation should arrive the earliest. Because of the larger absorption of the *o*-ray through the thick LC cell, however, the *o*-*o* component is not apparent in Fig. 4. The time delay between the *e*-*e* and *o*-*e* (or *e*-*o*) components was 2.735 ps, in good agreement with the theoretical value of 2.755 ps.

Compared with our previous work, the tuning range of the two-stage THz tunable LC Lyot filter was from 0.388 to 0.564 THz with an insertion loss of 8 dB. The tunable range of the THz LC Solc filter reported in this Letter can be tuned from 0.176 to 0.793 THz, and the insertion loss is about 5 dB. Moreover, two elements were needed in the Solc filter instead of the four elements used in the Lyot filter.

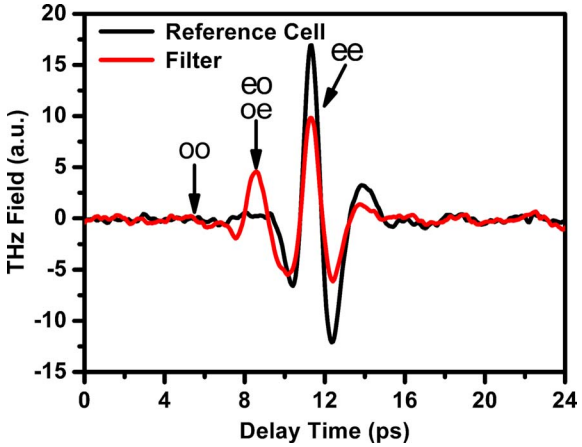

Fig. 4. (Color online) Temporal profile of a THz pulse transmitted through the LC Solc filter and reference LC cells.

Furthermore, phase retarders consisting of LC cells of different thicknesses are required for a Lyot filter, whereas the tunable LC phase retarders in the Solc filter were identical.

In summary, we have demonstrated for the first time (to our knowledge) a THz Solc filter using LC cells as the birefringent elements. The first central passband frequency of the filter can continuously be tuned from 0.176 to 0.793 THz, and the insertion loss is about 5 dB. The experimental data are in good agreement with theoretical predictions.

This work was supported in part by the Program for Promoting Academic Excellence of Universities (phase II) and grant NSC 95-2221-E-009-249 from the National Science Council as well as the Academic Top Universities program of the Ministry of Education, Taiwan.

References

1. P. F. Goldsmith, Proc. IEEE **80**, 1729 (1992).
2. M. Tonouchi, Nat. Photonics **1**, 97 (2007) and references therein.
3. I. H. Libon, S. Baumgärtner, M. Hempel, N. E. Hecker, J. Feldmann, M. Koch, and P. Dawson, Appl. Phys. Lett. **76**, 2821 (2000).
4. H. Nemec, P. Kuzel, L. Duvillaret, A. Pashkin, M. Dressel, and M. T. Sebastian, Opt. Lett. **30**, 549 (2005).
5. F. Yang and J. R. Sambles, Appl. Phys. Lett. **79**, 3717 (2001).
6. T. D. Drysdale, I. S. Gregory, C. Baker, E. H. Linfield, W. R. Tribe, and D. R. S. Cumming, Appl. Phys. Lett. **85**, 5173 (2004).
7. C.-L. Pan, C.-F. Hsieh, R.-P. Pan, M. Tanaka, F. Miyamaru, M. Tani, and M. Hangyo, Opt. Express **13**, 3921 (2005).
8. C.-Y. Chen, C.-L. Pan, C.-F. Hsieh, Y.-F. Lin, and R. P. Pan, Appl. Phys. Lett. **88**, 101107 (2006).
9. J.-L. Leroy, J. Opt. (Paris) **11**, 293 (1980).
10. I. Solc, J. Opt. Soc. Am. **55**, 621 (1965).
11. B. M. Schiffman and L. Young, IEEE Trans. Microwave Theory Tech. **16**, 351 (1968).
12. J. W. Evans, J. Opt. Soc. Am. **48**, 142 (1958).
13. D. A. Pinnow, R. L. Abrams, J. F. Lotspeich, D. M. Henderson, T. K. Plant, R. R. Stephens, and C. M. Walker, Appl. Phys. Lett. **34**, 391 (1979).
14. H. A. Tarry, Electron. Lett. **11**, 471 (1975).
15. A. Yariv and P. Yeh, *Optical Waves in Crystal: Jones Calculus and its Application to Birefringent Optical Systems* (Wiley, 1984).
16. C.-Y. Chen, C.-F. Hsieh, Y.-F. Lin, R. P. Pan, and C.-L. Pan, Opt. Express **12**, 2630 (2004).
17. F. J. Kahn, Appl. Phys. Lett. **22**, 386 (1973).
18. P. G. de Gennes and J. Prost, *The Physics of Liquid Crystals*, 2nd ed. (Oxford U. Press, 1983).